LysM receptor-like kinases involved in immunity perceive lipo-chitooligosaccharides in mycotrophic plants

Tongming Wang, Virginie Gasciolli, Mégane Gaston, Lauréna Medioni, Marie Cumener, Luis Buendia, Bingxian Yang, Jean Jacques Bono, Guanghua He, Benoit Lefebvre

LysM receptor-like kinases involved in immunity perceive lipo-chitooligosaccharides in mycotrophic plants

Running Title : **NbLYK4 is a LCO receptor modulating plant defense**

Tongming Wang[1,2], Virginie Gasciolli[2], Mégane Gaston[2], Lauréna Medioni[2], Marie Cumener[2], Luis Buendia[2], Bingxian Yang[3], Jean Jacques Bono[2], Guanghua He[1] and Benoit Lefebvre[2]

[1]Rice Research Institute, Key Laboratory of Application and Safety Control of Genetically Modified Crops, Academy of Agricultural Sciences, Southwest University, Chongqing 400715, China

[2]LIPME, Université de Toulouse, INRAE, CNRS, Castanet-Tolosan, France

[3]College of Life Sciences and Medicine, Zhejiang Sci-Tech University, Hangzhou, Zhejiang 310018, China

Corresponding authors and e-mail addresses: Benoit Lefebvre, benoit.lefebvre@inrae.fr and Guanghua He, heghswu@163.com

AUTHOR CONTRIBUTIONS

B.L. and J.J.B. designed experiments; T.W., V.G., M.G., L.M., M.C., L.B. performed experiments; B.Y. and G.H. analyzed the RNAseq data; B.L., T.W. and J.J.B analyzed the other data; B.L. and T.W. wrote the manuscript; G.H. and J.J.B edited the manuscript.

The author responsible for distribution of materials integral to the findings presented in this article in accordance with the policy described in the Instructions for Authors (https://academic.oup.com/plphys/pages/General-Instructions) is Benoit Lefebvre.

One-sentence summary

A group of LysM receptor-like kinases known to modulate plant defense is also involved in establishment of arbuscular mycorrhiza in plant species able to establish the latter symbiosis.

ABSTRACT

Symbiotic microorganisms such as arbuscular mycorrhizal fungi (AMF) produce both conserved microbial molecules that activate plant defense and lipo-chitooligosaccharides (LCOs) that modulate plant defense. Beside a well-established role of LCOs in activation of a signaling pathway required for AMF penetration in roots, LCO perception and defense modulation during arbuscular mycorrhiza is not well understood. Here we show that members of the LYRIIIA phylogenetic group from the multigenic Lysin Motif Receptor-Like Kinase family have a conserved role in dicotyledons as modulators of plant defense and regulate AMF colonization in the Solanaceae species *Nicotiana benthamiana*. Interestingly, these proteins have high-affinity for LCOs in plant species able to form a symbiosis with AMF but have lost this property in species that have lost this ability. Our data support the hypothesis that LYRIIIA proteins modulate plant defense upon LCO perception to facilitate AMF colonization in mycotrophic plant species and that only their role in plant defense, but not their ability to be regulated by LCOs, has been conserved in non-mycotrophic plants.

Keywords: Arbuscular Mycorrhizal Fungi (AMF); Symbiotic signal; Lipo-chitooligosaccharides (LCOs); Microbe-Associated Molecular Patterns (MAMPs); Defense; Lysin Motif Receptor-Like Kinase (LysM-RLK); Solanaceae

INTRODUCTION

Plants are permanently in contact with microorganisms, some of which are pathogenic while others are beneficial. Most often, pathogenic microorganisms first penetrate and then multiply in plant tissues. For example, pathogenic bacteria such as *Pseudomonas syringae* invade leaves through stomata and multiply between the mesophyll cells while *Ralstonia solanacearum* invades roots, penetrates in the vasculature and multiplies in the xylem. Similarly, beneficial microorganisms such as arbuscular mycorrhizal fungi (AMF) also penetrate in roots, propagate most often intercellularly, and colonize inner cortex cells in which they form a typical structure called an arbuscule, through which they exchange nutrients gathered in soil for plant sugars and lipids. It is thus essential for plants to discriminate friends and foes in order to mount appropriate responses such as expression/activation of the defense machinery or the AMF colonization machinery.

One layer of plant defense against pathogenic microbes involves perception by plants of conserved microbial signatures, called microbe-associated molecular patterns (MAMPs), and consequently induction of MAMP-triggered immunity (MTI). Well characterized MAMPs are flg22, a peptide derived from flagellin, the main component of the bacterial flagellum, which is perceived by the leucine-rich repeat (LRR) receptor-like kinase (RLK) FLS2 in Arabidopsis (*Arabidopsis thaliana*) (Gomez-Gomez and Boller, 2000; Chinchilla et al., 2006) and chitin fragments, derived from fungal cell walls which are perceived by the Lysin motif receptor-like protein (LysM-RLP) LYM2 and the LysM-RLKs LYK4, LYK5 and CERK1 in *A. thaliana* (Miya et al., 2007; Cao et al., 2014; Cheval et al., 2020). The chitin fragments that have the strongest defense elicitation activities are the chitooligosaccharides (COs) composed of 8 *N*-Acetyl Glucosamine (GlcNAc) residues. Typical responses to MAMPs are production of reactive oxygen species (ROS), MAP kinase phosphorylation and callose deposition on cell surfaces. Since MAMPs are conserved microbial signatures, they are not specific to pathogens and are also present in beneficial microbes. This is the case in AMF, which like all fungi, have chitinic cell walls. Thus, the plant defense machinery is activated during AMF colonization. Indeed, 40% of the genes induced by various pathogenic fungi in rice are also induced by AMF (Güimil et al., 2005) and well characterized pathogenesis related (PR) genes were found to be induced by AMF in rice (*Oryza sativa*), wheat (*Triticum aestivum*) and sorghum (*Sorghum bicolor*)(Campos-Soriano et al., 2012; Fiorilli et al., 2018; Watts-Williams et al., 2019). Strong defense reactions are observed in some plant mutants blocked in AMF colonization or

arbuscule formation (Chen et al., 2020). In wild type plants, defense responses can be modulated by the symbiotic partners. AMF produce numerous protein effectors, some of which were shown to interfere with the plant defense machinery (Kloppholz et al., 2011; Zeng et al., 2020). In addition, AMF produce Lipo-chitooligosaccharides (LCOs) that are acylated COs of 4-5 GlcNAc residues (Maillet et al., 2011). LCOs were originally identified in nitrogen-fixing rhizobial bacteria (reviewed in Fliegmann and Bono, 2015) and more recently in other fungi (Rush et al., 2020). They are essential for nitrogen-fixing symbiosis establishment in legumes (reviewed in Fliegmann and Bono, 2015) and also involved in AM establishment in both legumes and non-legumes (Feng et al., 2019; Girardin et al., 2019) through activating the common symbiosis signaling pathway required for root colonization by rhizobia and AMF. In addition, LCOs have been shown to interfere with the defense machinery in legumes (Shaw and Long, 2003; Liang et al., 2013; Feng et al., 2019; Rey et al., 2019) and in *A. thaliana* (Liang et al., 2013), although the latter does not form symbiosis either with rhizobia or with AMF. Two genes in tandem in the genomes of legumes and most dicots encode for high affinity LCO binding proteins (Broghammer et al., 2012; Fliegmann et al., 2013; Girardin et al., 2019) belonging to two LysM-RLK phylogenetic groups called LYRIA and LYRIIIA (Buendia et al., 2018). A LYRIA gene is found in most dicots and monocots. The LYRIA gene from the model legumes *Medicago truncatula*, *MtNFP*, or *Lotus japonicus, LjNFR5*, was shown to be required for symbiosis by rhizobia (Madsen et al., 2003; Arrighi et al., 2006). In addition, *MtNFP*, as well as LYRIA genes from Solanaceae, *SlLYK10* or *PhLYK10*, and from rice, *OsNFR5*/*OsMYR1*, were shown to be involved in symbiosis by AMF (Miyata et al., 2016; Feng et al., 2019; Girardin et al., 2019; He et al., 2019). Moreover, *MtNFP* was shown to be involved in plant defense against various types of pathogens (Ben et al., 2013; Rey et al., 2013) and in the interference between LCOs and the defense machinery (Feng et al., 2019). Interestingly, the LYRIA gene was lost during evolution in *A. thaliana* as well as in other species incapable of forming root endosymbioses (Delaux et al., 2014).

In contrast to the LYRIA group, a LYRIIIA gene is found in all dicots, including in species not forming root endosymbioses. The LYRIIIA gene of *A. thaliana*, *AtLYK4*, and of *L. japonicus*, *LjLYS12*, were shown to be involved in plant defense against various pathogens (Wan et al., 2012; Fuechtbauer et al., 2018). LYRIIIA proteins from most legumes, including *M. truncatula* (MtLYR3) and *L. japonicus* (LjLYS12), were found to exhibit a high affinity for LCOs in the nanomolar range, but not those of Lupinus species, which are rare cases of legumes unable to

establish symbiosis with AMF (Fliegmann et al., 2013; Malkov et al., 2016). Therefore, it is tempting to speculate that in mycotrophic plants, the LYRIIIA proteins could participate to the modulation of plant defense upon LCO binding to facilitate colonization by LCO-producing AMF. It is however unknown whether LYRIIIA genes play a role in AM and whether their LCO binding property and role in plant defense are conserved in mycotrophic non-legume species. To test this hypothesis, we have characterized the LYRIIIA gene from the mycotrophic Solanaceae *Nicotiana benthamiana* and studied the biochemical properties of orthologs from other mycotrophic and non-mycotrophic dicots. We found that the *N. benthamiana* LYRIIIA protein is a high affinity LCO binding protein regulating responses to the MAMP flg22 and colonization by both pathogens and AMF. The role in defense is conserved in the *A. thaliana* LYRIIIA gene but the encoded protein does not bind LCOs. We propose a model for the role of the LYRIIIA gene in modulation of the defense machinery and an evolutionary scenario for loss of LCO binding properties in non-mycotrophic species.

RESULTS

LCO binding properties of LYRIIIA proteins are conserved in mycotrophic non-legumes

LysM-RLKs of the LYRIIIA phylogenetic group from several mycotrophic legumes, but not those from non-mycotrophic Lupinus legume species, exhibit high affinity towards LCOs (Fliegmann et al., 2013; Malkov et al., 2016). Here, we extended our study to non-legume LYRIIIA proteins in order to determine whether the LCO binding properties are also shared by mycotrophic plants but not by non-mycotrophic ones. For this purpose, we cloned the LYRIIIA genes from the mycotrophic species peach (*Prunus persica*) (*PpLYR3*) which is phylogenetically closely related to legumes and *N. benthamiana* (*NbLYK4*) which is more phylogenetically distant, and from the non-mycotrophic species *A. thaliana* (*AtLYK4*). The LysM-RLK family from *N. benthamiana* is similar to that found in other Solanaceae (Supplemental Figure S1A-B; Buendia et al., 2016; Girardin et al., 2019), except that since *N. benthamiana* is an allotetraploid species, two homoeologous genes are found for almost all the LysM-RLKs present in other Solanaceae (Supplemental Figure S1A). Amino acid sequence alignment showed that the two *N. benthamiana* LYRIIIA proteins (NbLYK4.1 and NbLYK4.2) are very similar (95% identity, Supplemental Figure S1C-D). The percentage of identity between the LYRIIIA proteins from mycotrophic species is not high (about 55%, Supplemental Figure S1D) but is higher than the

one between these species and the non-mycotrophic species *A. thaliana* (about 45 %, Supplemental Figure S1D).

We used agrobacterium-mediated transient expression to produce NbLYK4.1, NbLYK4.2, AtLYK4 and PpLYR3 as C-terminal fusions with YFP in *N. benthamiana* leaves. By confocal microscopy, we found that all these proteins are localized at the cell periphery, as expected for putative plasma membrane proteins (Figure 1A and Supplemental Figure S2A). Each protein was immunodetected in the membrane fractions extracted from *N. benthamiana* leaves (Figure 1B and Supplemental Figure S2B). Their ability to bind LCOs was determined by radio-ligand binding assays. Equilibrium binding assays performed with LCO-V(C18:1,NMe,^{35}S) revealed specific binding of LCOs to membrane fractions prepared from leaves expressing NbLYK4.1-YFP, NbLYK4.2-YFP or PpLYR3-YFP but not from those expressing AtLYK4-YFP or in membrane fractions from untransformed leaves (Figure 1C and Supplemental Figure S2C-D). Since NbLYK4.1 and NbLYK4.2 are both able to bind LCOs and that *NbLYK4.2* has a higher transcript level (see below), we only used NbLYK4.2 for further characterization. Experiments performed on membrane fractions with a radioactive and photo-activatable LCO derivative showed photoaffinity labelling of NbLYK4.2-YFP and PpLYR3-YFP similar to MtLYR3-YFP (Figure 1D). Labelling to these proteins was inhibited by competition with an excess of unlabeled LCO. In contrast, the weak labelling observed on AtLYK4-YFP was not inhibited by an excess of unlabeled LCOs and thus corresponds to non-specific binding (Figure 1D). Absence of specific photoaffinity labelling on AtLYK4-YFP was confirmed by competition assays with a set of LCOs and COs (Supplemental Figure S2E). To characterize the LCO binding site of NbLYK4.2 and PpLYR3, we performed radiolabeled ligand binding assays with various unlabeled LCOs, including LCO-IV(C18:1,S) and LCO-IV(C18:1) found in AMF (Maillet et al., 2011), and COs as competitors (Figure 1E). Scatchard plot analysis of a cold saturation experiment with LCO-V(C18:1,NMe,S) revealed the presence of a single class of binding sites (Supplemental Figure S2F) with dissociation constants (K_d) of 18 nM ± 2 nM (n=3) and 8 nM ± 1 nM (n=3) for NbLYK4.2 and PpLYR3, respectively (Figure 1E). Inhibitory constants (K_i) were similar for the different LCOs tested, showing no selectivity of NbLYK4.2 and PpLYR3 for LCO structure (Figure 1E). In contrast, inhibitory constants (K_i) using CO4 or CO8 as competitors were higher than 1 µM, showing that the LCO binding site of NbLYK4.2 and PpLYR3 exhibits no or a much lower affinity for COs (Figure 1E). In conclusion, NbLYK4.2 and PpLYR3, but not AtLYK4, are high affinity LCO binding proteins and their binding sites discriminate LCOs versus COs.

***NbLYK4* regulates plant resistance to pathogens**

LYRIIIA genes were shown to be involved in plant defense against pathogens both in the legume *L. japonicus* and the non-legume *A. thaliana* (Wan et al., 2012; Fuechtbauer et al., 2018). Following our hypothesis that LYRIIIA proteins are involved in modulation of defense upon LCO perception, we expected LYRIIIA genes from mycotrophic non-legumes to be also involved in plant defense. We tested it in the Solanaceae *N. benthamiana* since it is more amenable than *P. persica* for genetic approaches. Transgenic *N. benthamiana* plants expressing an artificial microRNA (*amiR*) targeting both *NbLYK4.1* and *NbLYK4.2* genes (thereafter collectively referred as *NbLYK4*) were produced. *NbLYK4* relative expression level was strongly reduced in leaves and roots of two independent *N. benthamiana* lines *amiR1* and *amiR2* (Supplemental Figure S3A-C), while the relative expression level of the *NbLYK4* paralog with the highest percentage of nucleotide sequence identity, *NbLYK7* (55%), was not affected by the *amiR* (Supplemental Figure S3D-F). To confirm that any phenotype observed in the *amiR* lines was due to *NbLYK4*, we produced a complementation line, *amiRC*, by introducing additional WT copies of *NbLYK4.2*. *amiRC* showed partial recovery of *NbLYK4* expression level (Supplemental Figure S4).

To determine whether *NbLYK4* is involved in resistance to pathogens, we first tested plant susceptibility to the bacterial pathogen *Pseudomonas syringae*. We used a *P. syringae* DC3000 mutant in the HopQ avirulent gene (thereafter called ΔHopQ). This strain is pathogenic on *N. benthamiana* (Schultink et al., 2017). The kinetic of the ΔHopQ growth in 4-week-old WT *N. benthamiana* leaves showed a maximum at 3 dpi by dipping leaves in a bacterial solution (Supplemental Figure S5A). We thus measured bacterial density in leaves of *NbLYK4*-silenced plants at 2 dpi and found that bacterial density was significantly increased in *NbLYK4*-silenced plants compared to the controls (referring collectively to the WT, transgenic control and complemented lines; Figure 2A, Supplemental Figure S5B). This was confirmed by quantifying leaf symptoms at 2 dpi by ΔHopQ infiltration in leaves (Supplemental Figure S5C-E).

We also measured *N. benthamiana* susceptibility to the root pathogen, *Ralstonia solanacearum*. The percentage of plant survival after infection was significantly decreased in *NbLYK4*-silenced plants compared to WT plants (Supplemental Figure S6).

***NbLYK4* regulates plant response to MAMPs**

To better understand the increased susceptibility of *NbLYK4*-silenced plants to bacterial pathogens, we measured responses to the well-characterized bacterial MAMP flg22. Flg22-

induced ROS production and growth inhibition were significantly decreased in *NbLYK4*-silenced plants compared to controls (Figure 2B-C and Supplemental Figure S7A-F).

We then analyzed *NbLYK4* expression pattern in response to MAMPs. We measured by reverse transcription quantitative PCR (RT-qPCR) an induction of *NbLYK4* expression in *N. benthamiana* leaves 4 hours post infiltration of 10^{-7}M flg22 (Figure 2D). Similarly, strong GUS activity was observed all over leaves of *ProNbLYK4.1:GUS* transgenic plants treated with 10^{-7}M flg22 while basal expression was restricted to leaf vasculature (Figure 2E). Expression of *NbLYK4* was also induced in *N. benthamiana* leaves 4 hours post infiltration with the non-pathogenic bacteria *Pseudomonas fluorescens*. Interestingly *NbLYK4* expression was much less induced by infiltration of ΔHopQ than by infiltration of a *P. syringae* DC3000 mutant (ΔhrcC) that does not express the type III secretion system (Figure 2D), suggesting that *P. syringae* effectors can directly or indirectly inhibit *NbLYK4* expression.

We also performed messenger RNA sequencing of WT and *amiR1* plants (Supplemental Table S1-2). Expression of *NbLYK4.1* and *NbLYK4.2* was found to be decreased by about 60% in the *amiR1* plantlets used for RNAseq (Supplemental Table S3). We found 193 genes more expressed in WT (log2fold change >1.5) than in amiR plantlets and 359 genes less expressed in WT (log2fold change <-1.5) than in amiR plantlets (Supplemental Table S4). GO and KEGG term enrichment among these genes suggested that metabolism, in particular oxidative stress and photosynthesis are affected in the *NbLYK4*-silenced plants (Supplemental Figure S8, Supplemental Table S4). In addition, functions in signaling and plant pathogen interactions were found to be enriched in the differentially expressed genes (Supplemental Figure S8, Supplemental Table S4). Interestingly, expression of the *N. benthamiana* flg22 receptor, *NbFLS2* (Niben101Scf01785g10011; Hann and Rathjen, 2007; Hao et al., 2016) was not changed between the lines (Supplemental Table S2) suggesting an effect of *NbLYK4*-silencing on flg22 signaling rather than in flg22 perception.

Although NbLYK4.2 is a LCO binding protein while AtLYK4 is not, both *NbLYK4* and *AtLYK4* play a role in plant resistance to pathogens suggesting this role is conserved in mycotrophic and non-mycotrophic plants. To confirm it, we complemented the *Atlyk4-1* mutant with *NbLYK4.2-YFP* (and as a control *YFP* alone) expressed under the control of the constitutive Pro35S. We found in transgenic *Atlyk4-1* expressing YFP, a decrease of flg22-induced growth inhibition (Figure 2F), as observed in *NbLYK4*-silenced plants (Figure 2C). In *Atlyk4-1* expressing

NbLYK4.2-YFP (Figure 2F) the flg22-induced growth inhibition was similar to that of WT Col-0 suggesting that NbLYK4.2-YFP can complement *Atlyk4-1* for responses to flg22.

Conversely, *AtLYK4* was shown to modulate chitin signaling in *A. thaliana*. We tested whether *NbLYK4* also modulates chitin signaling in *N. benthamiana*. CO8-induced ROS production was significantly decreased both in leaves and roots of *NbLYK4*-silenced plants compared to controls (Figure 2G-H).

Altogether, these data showed that *NbLYK4* can modulate MAMP responses and resistance to pathogens in *N. benthamiana.*

LCOs modulate plant defense in the mycotrophic non-legume species *N. benthamiana*

LCO modulation of plant defense has been reported in legumes (Shaw and Long, 2003; Liang et al., 2013; Feng et al., 2019; Rey et al., 2019). Since our working hypothesis considers that LCO modulation of defense facilitates AMF colonization, we expected that exogenous LCO application would also modulate plant defense in non-legume mycotrophic plant species. We measured the interference of one of the LCOs produced by AMF, LCO-IV(C18:1,S) (Maillet et al., 2011) with several well characterized plant responses to the MAMP flg22 including responses ranging from minutes (ROS production and MAP kinase phosphorylation) to days (callose deposition and growth inhibition) after flg22 application. All responses to 10^{-8}M flg22 were significantly decreased in the presence of 10^{-7}M LCOs (Figure 3A-D and Supplemental Figure S9A). At 10^{-7}M flg22, an LCO effect was also observed on flg22-induced callose deposition and growth inhibition, but not on flg22-induced ROS production (Supplemental Figure S9B-H), suggesting that sensitivity of the defense responses to LCOs depends on whether they are short-term or long-term responses. In order to study the possible interference of LCOs with other MAMPs, we measured the level of ROS induced by 10^{-6}M CO8. ROS production was significantly decreased in the presence of 10^{-7}M LCOs (Figure 3E).

In conclusion, LCO ability to decrease MAMP-induced plant defense responses is conserved in a Solanaceae species phylogenetically distant from legumes.

Interestingly, the flg22-induced growth inhibition was reduced in LCO-treated WT or control plants but not in *NbLYK4*-silenced plants (Figure 3F). At the opposite, in *NbLYK4*-silenced plants, the LCO treatment resulted in a higher level of flg22-induced growth inhibition, an effect which was thus independent of *NbLYK4* but unmasked by *NbLYK4*-silencing.

***NbLYK4* regulates AM establishment**

Following our hypothesis that LYRIIIA proteins are involved in modulation of defense following LCO perception, to facilitate AMF colonization, we expected the LYRIIIA gene to regulate AMF colonization. We tested it in our *NbLYK4*-silenced plants. Both number of colonization sites (which quantifies early stage of colonization) and root colonization rate (which quantifies latter stage of colonization) were significantly increased in *NbLYK4*-silenced plants roots in comparison to the controls (Figure 4A-B, Supplemental Figure S10A). Furthermore, we measured the length of the colonized area at each colonization site and found that it was increased in the *NbLYK4*-silenced plants (Figure 4C). This suggests that AMF can penetrate and/or spread faster in roots of the amiR lines. As a complementary way to study the role of *NbLYK4* in AM, we produced transgenic lines overexpressing *NbLYK4-1* or *NbLYK4-2* (Supplemental Figure S4) and analyzed their AM phenotypes. Surprisingly, we also found an increase of AM colonization in these lines (Figure 4D). In order to confirm the AM phenotype, we measured the expression level of two AM marker genes (Rich et al., 2015) specifically expressed in mycorrhizal roots (Supplemental Figure S10B). We found that the two genes were all significantly more expressed in *NbLYK4*-silenced and overexpressing lines compared to control lines (Figure 4E). Similar effect of *NbLYK4* silencing and overexpression was consistent with a decrease of CO8-responses in both *NbLYK4*-silenced and overexpressing plants (Figure 2G-H, Supplemental Figure S10C).

We then analyzed *NbLYK4* expression pattern in roots during AM. For this, we grew the transgenic *N. benthamiana ProNbLYK4.1:GUS* line under sterile conditions with or without inoculation with AMF. GUS staining was observed all over the root system at 4wpi with AMF while almost no staining was observed in the non-inoculated plants (Figure 4F). GUS staining was associated with AMF colonization either in areas where only hyphae were growing (Figure 4G-H) and in areas where arbuscules were formed (Figure 4I-J).

Altogether, the data showed that *NbLYK4* expression is induced during AMF colonization and its function regulates AMF colonization.

DISCUSSION

In addition to controlling a plant machinery required for endosymbionts to colonize host roots (Fliegmann and Bono, 2015), LCOs modulate plant defense responses, but the molecular mechanisms involved in the latter response and their evolutionary origin are poorly understood. LCO modulation of plant defense was originally studied in legumes, because of

the potential role in the rhizobia symbiosis (Shaw and Long, 2003; Feng et al., 2019; Rey et al., 2019). A conserved role in non-legumes was suggested by observation of similar LCO effects in *A. thaliana*, although in this case it was not associated with symbiosis since this species does not form root endosymbioses (Liang et al., 2013). We found that LCO modulation of plant defense is conserved in mycotrophic non-legumes and we propose that the LYRIIIA LCO receptors modulate defense upon LCO perception to facilitate AMF colonization in mycotrophic species.

We showed that the LYRIIIA gene regulates defense against pathogenic bacteria in *N. benthamiana*. A pivotal role of *NbLYK4* in defense is reinforced by the observation that *P. syringae* effectors directly or indirectly regulate *NbLYK4* expression. This is consistent with data obtained on LYRIIIA genes from *L. japonicus* and *A. thaliana*. It appears that the role of LYRIIIA genes in defense is not restricted to one type of pathogens since LYRIIIA mutants were more susceptible to bacteria (*P. syringae* (our data and Wan et al., 2012) and *R. solanacearum* (our data)), a fungus (*Alternaria brassicicola* (Wan et al., 2012)) and an oomycete (*Phytophthora parasitica* (Fuechtbauer et al., 2018)). Moreover, *LYRIIIA* intervenes in resistance to pathogens in several plant organs since the above-mentioned pathogens include both root and leaf pathogens.

We showed that flg22 responses are partially suppressed in LYRIIIA mutants both in *N. benthamiana* and in *A. thaliana*. In contrast, no modulation of flg22 responses was found in roots of *L. japonicus* LYRIIIA mutants (Fuechtbauer et al., 2018). This could be explained by a low LYRIIIA basal expression level in roots as we observed in *ProNbLYK4:GUS* plants grown in sterile conditions. In addition to its role in flg22 responses, we found that *NbLYK4* is involved in chitin signaling, as previously found for the *A. thaliana* LYRIIIA gene, *AtLYK4* (Wan et al., 2012; Cao et al., 2014). Together, it suggests that LYRIIIA proteins are constitutive positive regulators of MTI. Therefore, the function of LYRIIIA proteins as general modulators of MTI rather than CO receptors as previously suggested for AtLYK4, is more plausible. Indeed, it was recently shown that AtLYK4 is not a CO binding protein (Del Hierro et al., 2021), while other LYRIIIA proteins were clearly demonstrated to be LCO binding proteins (Fliegmann et al., 2013; Malkov et al., 2016). The latter biochemical function is confirmed here for LYRIIIA proteins of the mycotrophic non-legume species *P. persica* and *N. benthamiana*. In contrast, AtLYK4, like the previously characterized LYRIIIA proteins from two Lupinus species (*Lupinus angustifolius* and *Lupinus atlanticus* ;Malkov et al., 2016) does not exhibit LCO binding activity. Interestingly,

A. thaliana, *L. angustifolius* and *L. atlanticus* are not able to establish AM. This strongly suggests that the LCO binding property of LYRIIIA is associated with a function in AM. Indeed, in *N. benthamiana LYRIIIA* knock-down and overexpressing plants, we observed an increase in AMF colonization. Although similar effect of silencing and overexpression is surprising, this is often observed for genes involved in signaling. The increased AMF colonization might be a consequence of the decreased defense in these lines. We found that *NbLYK4* expression in roots is induced during AMF colonization. In contrast to LYRIA genes (Rasmussen et al., 2016; Girardin et al., 2019), this was not specifically associated with arbuscule formation, but also with hyphal growth. Expression and function of LYRIA and LYRIIIA genes in AM might thus be different. Induction of LYRIIIA expression is also not restricted to AMF. We found patchy root staining in *ProNbLYK4:GUS* roots, even in absence of AMF, when plants were grown in non-sterile conditions (Supplemental Figure S10D). We also found *NbLYK4* expression induced by flg22 and bacteria in leaves. Similarly, *AtLYK4* expression was found induced by various MAMPs including COs (Wan et al., 2012), oligogalacturonides (Denoux et al., 2008) and flg22 (Denoux et al., 2008; Lyons et al., 2013). *NbLYK4* expression during AMF colonization might thus be the consequence of the perception by the host plant of MAMPs produced by AMF.

We propose a functional model that integrates all the above results (Figure 5A), in which LYRIIIA proteins are constitutive activators of MTI. Increased expression of *NbLYK4* after MAMP perception would stimulate defense responses. In the LYRIIIA mutants, the absence of constitutive activation of MTI would explain the decreased MAMP responses and increased susceptibility to pathogens. A similar reduced MTI activation would also occur upon LCO binding to LYRIIIA. Therefore, during AMF colonization (Figure 5B), MAMPs produced by AMF, including chitin oligomers, would activate defense and AMF LCOs would i) control the machinery required for root penetration and arbuscule formation via LYRIA proteins and ii) locally inhibit defense via LYRIIIA proteins.

In legumes LCO perception by LYRIA proteins is also inhibiting defense and LYRIA genes have a dual role in defense and symbioses (Ben et al., 2013; Rey et al., 2013; Feng et al., 2019). It needs to be determined whether this is also the case in non-legumes and how complementary is the defense modulation by LCO through LYRIA and LYRIIIA proteins.

From an evolutionary point of view, LYRIA and LYRIIIA proteins are encoded by genes in tandem in most dicots (Buendia et al., 2018), however these two genes are not the most closely related LYR genes (Supplemental Figure S1). Since they both can bind LCOs in different

species, it is likely that the ancestral LYR gene was a LCO binding protein. In dicots, both LYRIA and LYRIIIA have a dual role in defense and symbioses, so it could be speculated that the ancestral gene also had dual roles in defense and symbioses. In dicots, both LYRIA and LYRIIIA are associated with symbioses but their roles and evolution are different. In species not forming symbiosis either with rhizobia or with AMF, like *A. thaliana*, the LYRIA gene was lost whereas the LYRIIIA gene was conserved but the encoded protein lost its biochemical function of LCO binding. The increased susceptibility to pathogens observed in LYRIIIA knock-out or knock-down lines might explain that this gene cannot be easily lost. However, inhibition of defense by LCOs might represent an opportunity for pathogens able to produce LCOs to hijack plant defense. It is thus plausible that such a property was counter-selected in *A. thaliana* and other species in which it is not required for AM establishment. LCO binding to the *M. truncatula* LYRIIIA protein was demonstrated to occur on LysM3 (Malkov et al., 2016). A critical residue for LCO binding, Y228 in MtLYR3, is responsible in part for the loss of LCO binding in *L. angustifolius* LanLYR3 (Supplemental Figure S1C; Bouchiba et al., 2022). This residue is an F in AtLYK4 as in NbLYK4.1 and NbLYK4.2, and thus cannot explain the loss of LCO binding in AtLYK4. Two additional residues important for LCO binding, T2019 and Q224 in MtLYR3 (Bouchiba et al., 2022) are different between AtLYK4 and the LCO binding LYRIIIA proteins, and could be involved in the loss of LCO binding in AtLYK4. Other residues that are not conserved in AtLYK4 while they are conserved among the LCO binding LYRIIIA proteins (Supplemental Figure S1C), might also be responsible for the inability of AtLYK4 to bind LCOs. Surprisingly, despite the absence of LYRIA protein and of LCO binding property of LYRIIIA in *A. thaliana*, LCOs can still modulate defense responses in this species (Liang et al., 2013). This effect was suggested to rely on another LysM-RLK, AtLYK3, that belongs to the LYKIII phylogenetic group. It remains to be determined whether LYKIII proteins have a similar role in mycotrophic plants and whether LYKIII proteins act in a parallel pathway or form a receptor complex with LYRIIIA proteins. The complexity of defense modulation by LCOs highlights the importance of fine tuning in the regulation of defense responses in order to allow symbioses to occur while maintaining resistance to pathogens.

MATERIALS AND METHODS

Plant growth conditions

Nicotiana benthamiana and Arabidopsis (*Arabidopsis thaliana*) seeds were surface sterilized with bleach solution (3.8% (v/v) and 2.5% (v/v) of active chloride for 20 min and 2min, respectively), rinsed three times with sterile water, transferred onto petri dishes containing MS (or ½ strength MS (1/2 MS) with 1% (w/v) sucrose for flg22-induced growth-inhibition assays) and placed in a growth chamber (21°C, 16h:8h, day:night photoperiod) for germination.

For the flg22-induced growth inhibition assays, 5-day-old *N. benthamiana or A. thaliana* plantlets were transferred into 48-well plates containing 600 µL of liquid 1/2 MS with 1% (w/v) sucrose and 10^{-7}M flg22 and 10^{-7}M chemically synthesized LCO-IV(C18:1,S) (Maillet et al., 2011) or corresponding amount of LCO solvent (LCO stock at 10^{-4}M stored in 50% (v/v) Acetonitrile), and cultured at 21°C (16h:8h, day:night photoperiod). For the CO8-induced ROS production assay in roots, 7-day-old *N. benthamiana* plantlets were transferred in magenta box containing sterilized attapulgite (Oil Dri, UK) irrigated with water and cultured at 25°C (16h:8h, day:night photoperiod). For AM analysis, 7-day-old *N. benthamiana* plantlets were transferred in pots containing sterilized attapulgite irrigated first with ½ modified Long Ashton medium (7.5 µM NaH_2PO_4), then with water and cultured at 21°C (16h:8h, day:night photoperiod).

For all the other assays on 4-week-old plants, 7-day old *N. benthamiana* plantlets were transferred on pots containing potting soil (SB2, Prooven) and cultured for 3 weeks at 21°C (16h:8h, day:night photoperiod).

Cloning

PpLYR3 (Prupe.7G147600), *NbLYK4.1* (Supplemental Table S5), *NbLYK4.2* (Supplemental Table S5) and *AtLYK4* (At2g23770) coding sequences were amplified by PCR from genomic DNA of *P. persica*, *N. benthamiana* and *A. thaliana* respectively (Primers listed in Supplemental Table S6) and inserted by Gateway cloning into a modified Pbin vector in translational fusion with YFP and under the control of *Pro35S*, as described in (Lefebvre et al., 2010). The *Pro35S*:*MtLYR3*-*YFP* construct is from (Fliegmann et al., 2013).

An artificial microRNA precursor based on the *M. truncatula* miR171 sequence was created by annealing two complementary short DNA sequences (Supplemental Figure S11). The amiR was inserted by Golden gate cloning into a modified pCambia 2200 vector(Fliegmann et al., 2016) to be expressed *in planta* under the control of *Pro35S*.

NbLYK4.1 promoter region (-1821 to -18 before ATG) and *NbLYK4.2* promoter region (-1180 to -7 before ATG) were amplified by PCR (Primers listed in Supplemental Table S6) from *N. benthamiana* genomic DNA and inserted by Golden Gate cloning into a modified pCambia 2200 vector (Fliegmann et al., 2016) in transcriptional fusion with the GUS reporter gene as described in (Girardin et al., 2019) or into a modified Pbin vector vector (Fliegmann et al., 2016) in transcriptional fusion the *NbLYK4.2* coding sequence. The construct *ProNbLYK4.2:NbLYK4.2* was then subcloned in the pCambia1390 vector using ScaI and SnaBI restriction enzymes.

Generation of transgenic *N. benthamiana* and *A. thaliana* lines

Transient expression in *N. benthamiana* leaves was performed with *Agrobacterium tumefaciens* LBA4404 virGN54D strains as described in (Mbengue et al., 2010). Leaves were harvested 3 days after infiltration.

Stable transformation of *N. benthamiana* (WT or amiR1) and *A. thaliana Atlyk4-1* (CS850683; Col-0 background; Wan et al., 2012) mediated by *A. tumefaciens* through callogenesis and floral dipping respectively was used to generate transgenic plants (T0) transformation. Two WT *N. benthamiana* lines containing the amiR (*amiR1* and *amiR2*) were selected first by screening *NbLYK4*-silencing level by RT-qPCR on T0 and T1 and then by screening survival on 100 mg/L kanamycin on T2 (to select homozygous lines). For these two lines, phenotyping was performed on T2 plants. One *N. benthamiana* line containing the *ProNbLYK4.1:GUS* construct was selected by screening survival on 100 mg/L kanamycin. This line was used for analysis of NbLYK4 expression pattern and as transgenic control in all phenotyping experiments. One *N. benthamiana* line containing the amiR and the *ProNbLYK4.2:NbLYK4.2* construct (*amiRC*) was selected by screening survival on 100 mg/L kanamycin and 50 mg/L hygromycin. Two *N. benthamiana* lines containing the *Pro35S:NbLYK4.2-YFP* or *Pro35S:NbLYK4.1-YFP* constructs (OE) were selected by screening survival on 100 mg/L kanamycin and level YFP fluorescence in the leaves. For these four lines, phenotyping was performed on T1 plants. *Atlyk4-1*/*Pro35S:YFP* and *Atlyk4-1*/*Pro35S:NbLYK4.2YFP* were selected by microscopy based on observation of YFP fluorescence. Phenotyping was performed on T2 plants.

LCO binding assays

Membrane fraction, SDS-PAGE and LCO binding assays were performed as described in (Girardin et al., 2019). LCO photoaffinity labelling was performed as described in (Fliegmann et al., 2013) except that crosslinking was made on purified proteins rather than on membrane

fractions. Protein purification was performed as described in (Lefebvre et al., 2012) using anti-GFP beads (Chromotek, Germany). LCO-V(C18:1,NMe,S) was purified from *Rhizobium tropici*. LCO-IV(C18:1,S), LCO-IV(C18:1), LCO-IV(C16:2,S), CO4 and CO8 were synthesized by CERMAV (Grenoble).

RNA isolation and gene expression analysis

Total RNA of plantlets, leaves or roots was isolated using RNAeasy plant mini kit (Qiagen). DNAse treatment was performed using the Turbo DNase kit (Ambion) after elution from columns. The integrity and quantity of the RNA preparations were verified using Agilent RNA 6000 Nano Chips (Agilent Technologies, USA). For RT-qPCR, complementary DNA synthesis was performed on of RNA and polyT primer using SuperScript II (Invitrogen, USA). LightCycler 480 SYBR Green I Master was used to achieve RT-qPCR on a LightCycler 480 (Roche, Switzerland) with the primers listed in Supplemental Table S6. Gene expression levels were calculated relative to the four *N. benthamiana* housekeeping genes listed in Supplemental Table S6.

RNAseq was performed on pools of 10 plantlets. The construction of transcriptome libraries and deep sequencing were performed by the Novogene Corporation (Beijing, China). Briefly, mRNA was purified from total RNA and fragmentation was performed. cDNA was amplified using random hexamer primers on fragmented RNAs. Phusion High-Fidelity DNA polymerase, Universal PCR primers and Index (X) Primer (Illumina) were used for PCR. The PCR products were purified (AMPure XP system) and library quality was assessed on the Agilent Bioanalyzer 2100 system. After cluster generation, the library preparations were sequenced on an Illumina Novaseq platform. Raw data have been deposited in the SRA database (accession number: PRJNA694786). Clean 150 bp paired-end reads were obtained by removing reads containing adapter, reads containing poly-N and low-quality reads through in-house perl scripts. Gene annotation was performed through mapping the clean reads to the reference genome (ftp://ftp.solgenomics.net/genomes/Nicotiana_benthamiana) by Hisat2 v2.0.5 (Mortazavi et al., 2008). RSeQC v2.3.6 (Wang et al., 2012) was used to calculate read-mapping statistics (Supplemental Table S1) for each sample from BAM files generated from SAMtools (Li et al., 2009). featureCounts v1.5.0-p3 (Liao et al., 2014) was used to count the read numbers mapped to each gene (Supplemental Table S2). Reads overlapping more than one gene were not counted. DESeq2 R package (1.16.1) was used for differential expression analysis (Anders and Huber, 2010; Love et al., 2014). The resulting *p*-values were adjusted using the Benjamini

and Hochberg's approach for controlling the false discovery rate (Robinson et al., 2010). Functional enrichment analysis of differentially expressed genes were implemented by the clusterProfiler R package, by using the GO and KEGG databases, respectively (Yu et al., 2012).

Quantification of MAPK phosphorylation and ROS production

Leaf discs and root fragments of 0.5 cm from 4-week old *N. benthamiana* plants were incubated in 96-well plates on deionized water for leaf discs or on 0.05% (v/v) EtOH for root fragments for 4h in darkness, then pretreated for 2 hours with 10^{-7}M LCO-IV(C18:1,S) or corresponding amount of LCO solvent when indicated. For ROS production assays, leaf discs and root fragments were incubated in the indicated flg22, CO8 and LCO-IV(C18:1,S) treatment, 20 µg/ml HRP and 0.34 mg/ml luminol (Aldrich, USA) for leaf discs, or 0.062 mg/ml (L-0.12 WAKO, Germany) for root fragments). Plates were immediately placed in a luminometer (FLUOstar Omega, Germany). The luminescence was recorded in each well during 400 milliseconds every minute. When LCO effect was tested, corresponding amount of LCO solvent was added with flg22 or CO8. For MAPK phosphorylation assays, water from petri dishes was removed and replaced by 10^{-8}M flg22 and 10^{-7}M LCO-IV(C18:1,S) or 10^{-8}M flg22 and corresponding amount of LCO solvent. Discs were harvested after 15 min and placed in 2 ml tube containing 150 µl/100 mg Laemmli buffer supplemented with protease inhibitors (0.1 mM AEBSF, and 1mg/mL each of leupeptin, aprotinin, antipain, chymostatin, and pepstatin) and phosphatase inhibitors (sodium fluoride, beta-glycerophosphate, sodium pyrophosphate, sodium orthovanadate). Total proteins were separated by SDS-PAGE and MAPK phosphorylation revealed using anti-phospho MAPK (p44/42 MAPK, Erk1/2); Cell signaling Technology, USA).

Quantification of callose deposition

Four-week-old *N. benthamiana* leaves were first infiltrated with 10^{-7}M LCO-IV(C18:1,S) or water with corresponding amount of LCO solvent, then with 10^{-7}M flg22 and 10^{-7}M LCO-IV(C18:1,S) or 10^{-7}M flg22 and water with LCO solvent. Leaves were harvested 48h later, incubated successively in 100% (v/v) boiling ethanol for 3min, in 75% (v/v) ethanol for 15 min, in 50% (v/v) ethanol for 15 min, in 150 mM phosphate buffer pH 8.0 for 15min, and finally stained with 0.05% (w/v) aniline blue in 150 mM phosphate buffer pH 8.0 overnight at 4°C. Grey-level images were acquired with a fluorescence microscope using a DAPI filter. Total callose deposition and number/area of callose deposits were respectively analyzed using the functions "mean grey value" and "particle analysis" of ImageJ. For images shown in

Supplemental Figure S3, leaves were directly infiltrated with 0.01% (w/v) aniline blue in 150 mM phosphate buffer pH 8.0 without ethanol clearing and imaged 48h later using a SP8 confocal microscope (Leica, Germany) with excitation at 405 nm and emission between 430-550 nm (laser intensity: 20%, PMT gain: 725, objective: 10x/0.30 dry).

Pathogen assays

Bacterial strains *Pseudomonas syringae* pv. tomato DC3000 ΔHopQ-DeltaFliC (ΔHopQ) and ΔhrcC (ΔT3SS) and *Pseudomonas fluorescens* were grown overnight at 28°C as liquid culture in King's B medium supplemented with 6 mM $MgSO_4$ and antibiotics specific for each strain (10 mg/L rifampicin and 100 mg/L ampicillin for *P. syringae ΔHopQ*; 50 mg/L rifampicin and 50 mg/L chloramphenicol for *P. syringae ΔT3SS*; 5 mg/L tetracycline and 15 mg/L chloramphenicol for *P. fluorescens*). Bacteria were collected, washed, and diluted to the desired OD_{600} with water. When bacteria were inoculated by dipping, 0.01% (v/v) silwet L-77 was added. To quantify bacterial growth, four discs / leaf (using same leaves on different plants) were placed in 1.5 ml tubes and manually ground with a plastic pestle in 0.1M PBS pH 6.8. The homogenate was diluted with water and distributed on petri dishes using an automatic plater (easySpiral, interscience, France) on plates containing King's B medium with antibiotics.

Ralstonia solanacearum GRS473 (Poueymiro et al., 2009) was grown overnight at 28°C in BG liquid medium (Plener et al., 2010) supplemented with 40 mg/L spectinomycin and 10 mg/L gentamicin. Root inoculation was performed on 2-week-old *N. benthamiana* plants by soil drenching with a 50 ml bacterial suspension at OD_{600}=0.1. Visual scoring of plant symptoms was performed according to a scale ranging from '0' (no symptoms) to '4' (complete wilting) as described in (Poueymiro et al., 2009). The disease scoring was then transformed into binary data, with a disease index below '2' as '0' and a disease index equal to or higher than '2' as '1'. Statistical analysis was performed as described in (Remigi et al., 2011).

AMF and GUS staining

Plantlets were inoculated with 200 or 500 spores (depending on the experiments) of *Rhizophagus irregularis* DAOM197198 spore stock solution (Agronutrition, France) diluted in modified Long Ashton medium.

For quantification of AMF colonization, root systems were immersed in 10% KOH (w/v) for 5min at 95°C, then stained by 5% (v/v) ink-vinegar solution for 5 min at 95°C. For quantification of early stages of AMF colonization, the total number of colonization sites was counted on

entire root systems. A colonization area with several neighboring arbuscules was considered as a colonization site. The width of colonization area was quantified by the software ImageJ on images acquired with an Axiozoom V16 (Zeiss, Germany). For quantification of later stages of AMF colonization, root colonization was estimated by the grid intersect method.

For GUS and AMF staining, root systems were first stained at 37°C overnight with 2% (w/v) X-Gluc in 0.2 M PBS pH 7.2 containing 1 mM EDTA, 5 mM potassium ferricyanide and 5 mM potassium ferrocyanide. Root systems were then treated with 100% (v/v) ethanol for 4h at room temperature and 10% KOH (w/v) for 8 min at 95°C. AMF were finally stained with 1 µg/ml WGA CF488A conjugate (Biotum, USA) in 0.2M PBS pH 7.2, triton-X100 0.01% (v/v), overnight at room temperature.

GUS staining in leaves was performed as for roots except that leaves were then cleared by incubation in 100% (v/v) ethanol for 4h, 70% (v/v) ethanol for 4h and 50% (v/v) ethanol over night at 37°C. GUS staining in leaves and roots was imaged with an Axiozoom V16 (Zeiss, Germany).

Sequence and statistical analyses

Protein alignment and calculation of AA identity were made by Clustal omega (www.ebi.ac.uk/Tools/msa/clustalo). Phylogenetic tree was calculated by PhyML and drawn by TreeDyn (www.phylogeny.fr). Statistical analyses were performed with Prism version 5.0 (GraphPad Software, USA).

Accession Numbers

Sequence data from this article can be found in the GenBank/EMBL data libraries under accession numbers Prupe.7G147600 (*PpLYR3*), At2g23770 (*AtLYK4*), Medtr5g019050 (*MtLYR3*) or on www.solgenomics.net (see *N. benthaminia* LysM-RLK accession numbers in Supplemental Figure S1).

Supplemental Data

Supplemental Figure S1. Phylogenetic tree of *N. benthamiana* LysM-RLK family.
Supplemental Figure S2. NbLYK4 and PpLYR3 but not AtLYK4 bind LCOs.

Supplemental Figure S3. *NbLYK4* but not its closest paralog *NbLYK7* is silenced by an artificial microRNA (amiR).
Supplemental Figure S4. *NbLYK4* expression in *amiRC* and OE lines.
Supplemental Figure S5. *NbLYK4*-silenced plants show increased susceptibility to *P. syringae* ΔHopQ.
Supplemental Figure S6. *NbLYK4*-silenced plants show increased susceptibility to *Ralstonia solanacearum*.
Supplemental Figure S7. *NbLYK4*-silenced plants show decreased flg22 responses.
Supplemental Figure S8. GO and KEGG term enrichment in the RNAseq DEGs.
Supplemental Figure S9. LCOs decrease flg22 responses.
Supplemental Figure S10. *NbLYK4* regulates AM symbiosis.
Supplemental Figure S11. amiR sequence

FUNDING

T.W.'s fellowship was funded by the "China Postdoctoral Science Foundation" (Grant No. 2018M643392) and the "Fundamental Research Funds for the Central Universities" (Grant No. XDJK2019C040). This work was supported by the "Innovative Research Groups" of Chongqing Natural Science Foundation (Grant NO. cstc2021jcyj-cxttX0004), the ANR projects "LCOinNONLEGUMES" (ANR-2010-JCJC-1602-01) and "WHEATSYM" (ANR-16-CE20-0025-01) and is set within the framework of the "Laboratoires d'Excellences (LABEX)" TULIP (ANR 10 LABX 41) and of the "École Universitaire de Recherche (EUR)" TULIP GS (ANR 18 EURE 0019).

ACKNOWLEDGMENTS

We thank Christine Faulkner (JIC, Norwich, UK) for providing *Atlyk4-1* seeds, and Nemo Peeters (LIPME, Toulouse, France) and Alan Collmer (Cornell University, Ithaca, USA) for the *Ralstonia solanacearum* and *Pseudomonas syringae* strains, respectively. We also thank Guojian Hu and Yi Chen (GBF, Toulouse, France) and Nemo Peeters for technical advices and Julie Cullimore and Judith Fliegmann for critical reading of the manuscript.

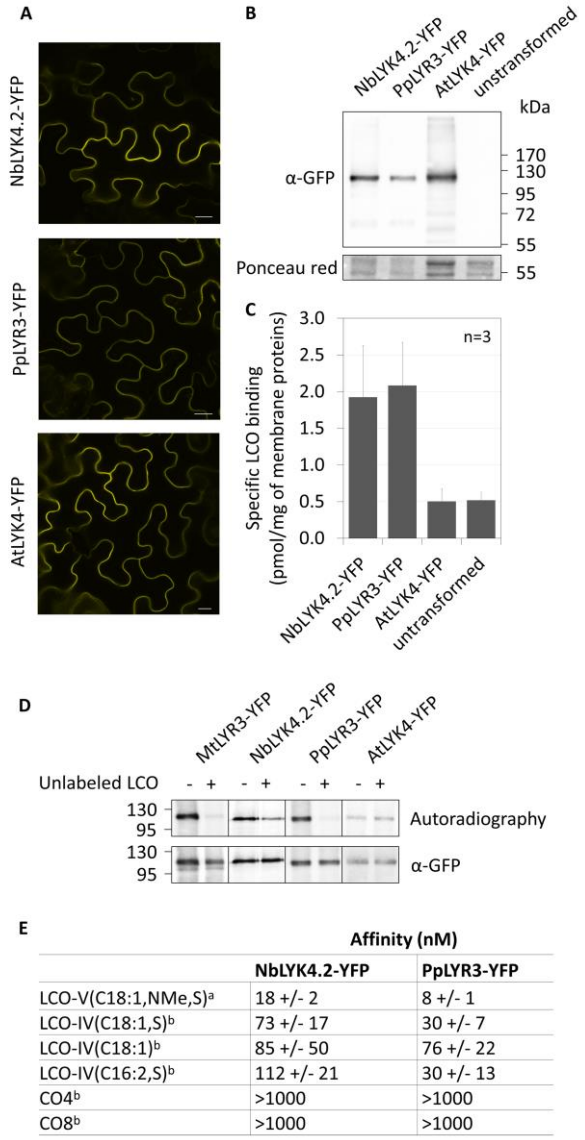

E

	Affinity (nM)	
	NbLYK4.2-YFP	**PpLYR3-YFP**
LCO-V(C18:1,NMe,S)[a]	18 +/- 2	8 +/- 1
LCO-IV(C18:1,S)[b]	73 +/- 17	30 +/- 7
LCO-IV(C18:1)[b]	85 +/- 50	76 +/- 22
LCO-IV(C16:2,S)[b]	112 +/- 21	30 +/- 13
CO4[b]	>1000	>1000
CO8[b]	>1000	>1000

Figure 1. LYRIIIA proteins are LCO binding proteins in mycotrophic plants

(A) Confocal images of *N. benthamiana* leaf epidermal cells transiently expressing the indicated YFP-fusion proteins. Scale bars represent 20 µm. **(B)** Immunodetection of the indicated transiently expressed YFP-fusion proteins in membrane fractions using anti-GFP antibodies. The Ponceau red staining shows the amounts of proteins on the immunoblots (corresponding to 10µg membrane protein used for SDS-PAGE). **(C)** Binding of LCO-V(C18:1,NMe,^{35}S) to the same membrane fractions used for immunoblotting in B. The means and standard deviations between three LCO-binding assays on the same membrane fraction. Biological replicates are shown in Supplemental Figure S2D. **(D)** Photoaffinity labelling of immunopurified indicated YFP-fusion proteins, using a radiolabeled- and photoactivatable-LCO derivative in absence or presence of 2 µM of unlabeled LCO-IV(C16:2,S). Autoradiography was performed on the same nitrocellulose membrane used for immunodetection with anti-

GFP antibodies. **(E)** Affinity (nM) of NbLYK4.2 and PpLYR3 for various LCOs and COs determined by cold saturation[a] (K_d) or competitive inhibition[b] (K_i) of LCO-V(C18:1,NMe,^{35}S) binding to the membrane fraction. Values are the means +/- standard deviations obtained from three independent batches of membrane fractions.

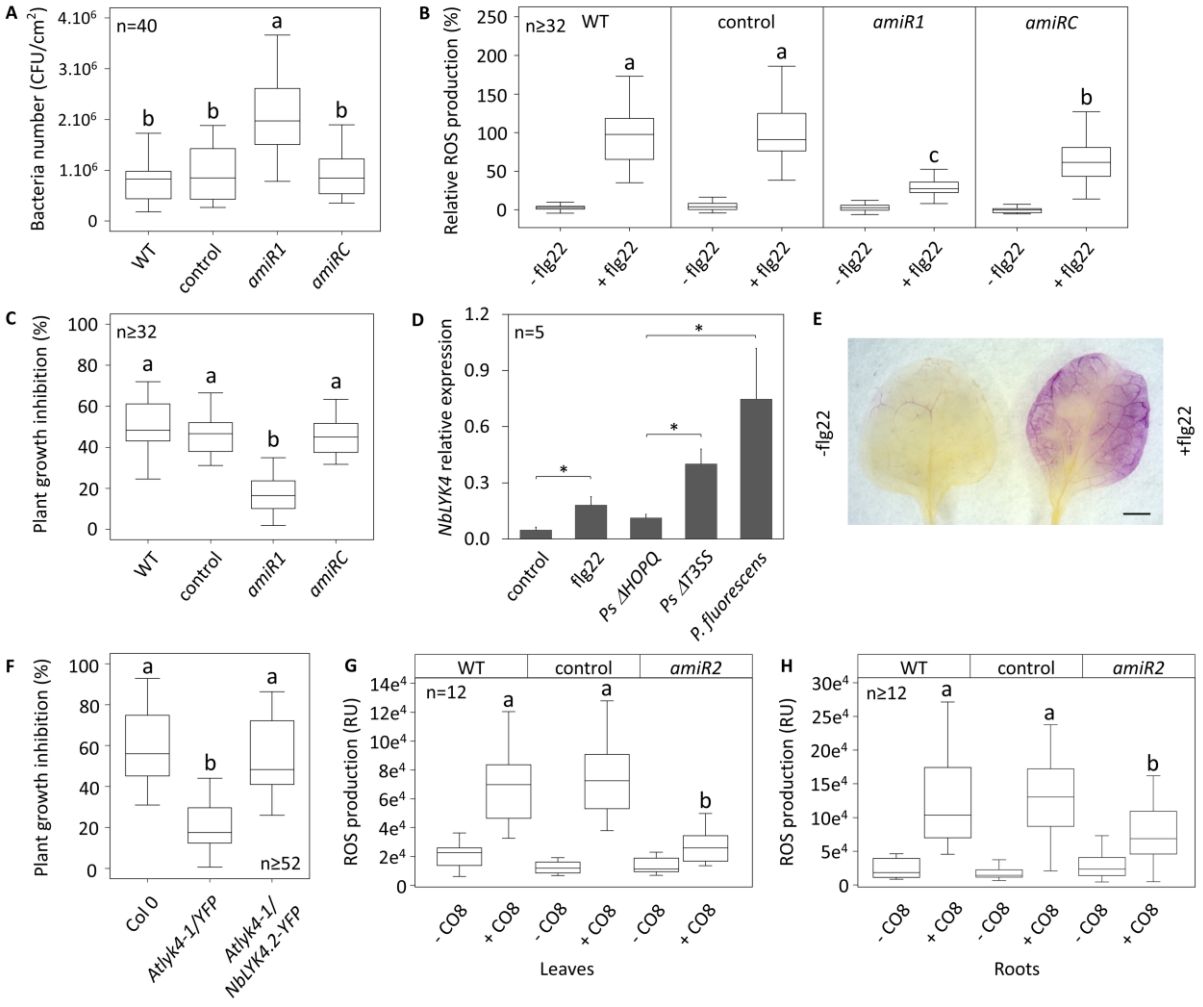

Figure 2. *NbLYK4* modulates MTI and its expression is regulated by a MAMP

(A) Growth of *Pseudomonas syringae* is increased in *NbLYK4*-silenced plants. *P. syringae* was inoculated by dipping leaves of 4-week-old *N. benthamiana* WT, control (transgenic control line), *amiR1* (*NbLYK4*-silenced line) and *amiRC* (*amiR1* complemented line) plants on a suspension at OD_{600}=0.01. Bacteria numbers were quantified by counting the colony-forming units (CFU) at 2 days post inoculation. Box plots represent the bacteria number in a total of 40 plants from 4 independent experiments. Center lines show the medians, box limits the upper and lower quartiles, and whiskers 1.5x the interquartile range. Different letters indicate significant differences between the lines ($P < 0.05$, Kruskal-Wallis test). **(B)** ROS production induced by flg22 is decreased in *NbLYK4*-silenced plants. Leaf discs of 4-week-old *N. benthamiana* were treated with 10^{-7}M flg22. Total H_2O_2 production for each leaf disc was normalized to the average for the WT+flg22 condition in each experiment. Box plots represent the H_2O_2 production in a total of 30 to 36 leaf discs from 6 independent experiments. Box plots as in A. Different letters indicate significant differences between the lines treated with flg22

(P < 0.05, ANOVA). Typical ROS production kinetics in the various lines are shown in Supplemental Figure S7A. **(C)** Growth inhibition induced by flg22 is decreased in *NbLYK4*-silenced plants. Five-day-old *N. benthamiana* plantlets were grown for two weeks in MS medium containing 10^{-7}M flg22. Box plots represent the growth inhibition (fresh weight of treated/non-treated plantlets) of a total of 32 to 48 plantlets from three independent experiments. Box plots as in A. Different letters indicate a significant difference between the lines (P < 0.05, Kruskal-Wallis test). Note that plantlet sizes were not difference before the flg22 treatment (Supplemental Figure S7E). **(D)** *NbLYK4* expression is induced by flg22 or by *Pseudomonas*. *NbLYK4* expression was measured by RT-qPCR in leaves of wild type *N. benthamiana* 4h after infiltration of 10^{-7}M flg22 or *P. syringae (Ps)* / *P. fluorescens* at OD_{600}=0.1 and normalized by the expression of four reference genes. Means and standard deviations between 5 independent experiments are shown. * indicate significant differences (P < 0.05, Pairwise T-test). **(E)** GUS activity (magenta) in *N. benthamiana* leaves from *ProNbLYK4.1:GUS* plants 4h after infiltration of 10^{-7}M flg22 (+flg22) or water (-flg22). Scale bar represents 1 cm. **(F)** Growth inhibition induced by flg22 is decreased in *Atlyk4-1* and this phenotype is complemented by *NbLYK4*. Five-day old Arabidopsis plantlets were grown for 12 days in MS medium containing 10^{-7}M flg22. Box plots represent the growth inhibition (fresh weight of treated/non-treated plantlets) in a total of 52 to 56 plantlets from three independent experiments. Box plots as in A. Different letters indicate a significant difference between the lines (P < 0.05, Kruskal-Wallis test). (G-H) ROS production induced by CO8 is decreased in *NbLYK4*-silenced plants. Leaf discs (G) or root fragments (H) of 4-week-old *N. benthamiana* plants were treated or not with 10^{-6}M CO8. Box plots represent the total H_2O_2 production in leaf discs or root fragments from at least 2 independent experiments. Box plots as in A. Different letters indicate significant differences between the lines treated with CO8 (P < 0.05, Pairwise T-Test).

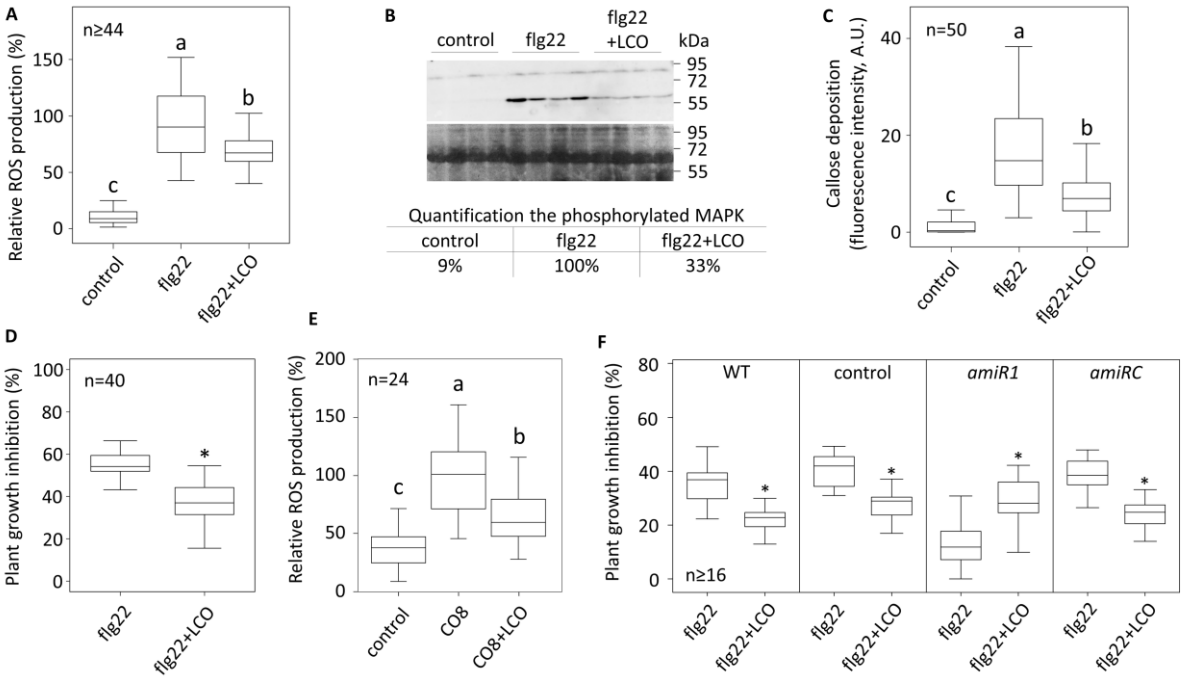

Figure 3. LCOs modulate flg22 responses in *N. benthamiana*

(A) LCOs decrease flg22-induced reactive oxygen species (ROS) production. Four-week-old WT *N. benthamiana* leaf discs were used to measure H_2O_2 production in response to 10^{-8}M flg22 with or without 1h pretreatment with 10^{-7}M LCOs. Total H_2O_2 production for each leaf disc was normalized by the average for the flg22 condition in each replicate. Box plots represent the total H_2O_2 production of a total of 44 to 48 leaf discs from 4 independent experiments. Center lines show the medians, box limits the upper and lower quartiles, and whiskers 1.5x the interquartile range. Different letters indicate significant differences between the treatments (P < 0.05, Kruskal-Wallis test). **(B)** LCOs decrease flg22-induced MAPK phosphorylation. Four-week old WT *N. benthamiana* leaves were used to measure MAPK phosphorylation 15 min after a 10^{-8}M flg22 treatment with or without 2h pretreatment with 10^{-7}M LCOs. Immunoblotting was performed on 4 samples per treatment, using anti phosphor-MAPK. The Ponceau red staining shows the amounts of proteins (corresponding to 10mg of leaf extract) used for SDS-PAGE. **(C)** LCOs decrease flg22-induced callose deposition. Four-week-old WT *N. benthamiana* leaves were used to measure callose deposition in response to 10^{-7}M flg22 with or without 24h pretreatment with 10^{-7}M LCOs. Callose was stained by aniline blue 48h post treatment with flg22 and imaged by fluorescence microscopy and quantified with ImageJ. Box plots represent the mean fluorescence intensity in a total of 50 images from 5 independent experiments. Box plots as in A. Different letters indicate significant differences between the treatments (P < 0.05, Kruskal-Wallis test). **(D)** LCOs

decrease flg22-induced plant growth inhibition. Five-day old WT *N. benthamiana* WT plantlets were incubated on MS medium containing either 10^{-7}M flg22 or a combination of 10^{-7}M LCOs and 10^{-7}M flg22. Growth inhibition ratio (fresh weight of treated/non-treated plantlets) was measured after two weeks. Box plots represent the plant growth inhibition ratio of a total of 40 plantlets from three independent experiments. Box plots as in A. * indicates a significant difference ($P < 0.05$, T-test). **(E)** LCOs decrease CO8-induced ROS production. Same as in (A) except that 10^{-6}M CO8 was used instead of 10^{-8}M flg22. Box plots represent the total H_2O_2 production of a total of 24 leaf discs from three independent experiments. Box plots as in A. Different letters indicate significant differences between the treatments ($P < 0.05$, Kruskal-Wallis test). **(F)** *NbLYK4*-silenced plants do not show decrease of flg22-induced plant growth inhibition in the presence of LCOs. Box plots represent the plant growth inhibition (fresh weight of treated/non-treated plantlets) of a total of 16 to 32 plantlets. * indicate significant differences ($P < 0.05$, T-test). Two additional experiments were performed and showed similar results (Supplemental Figure S7C-D).

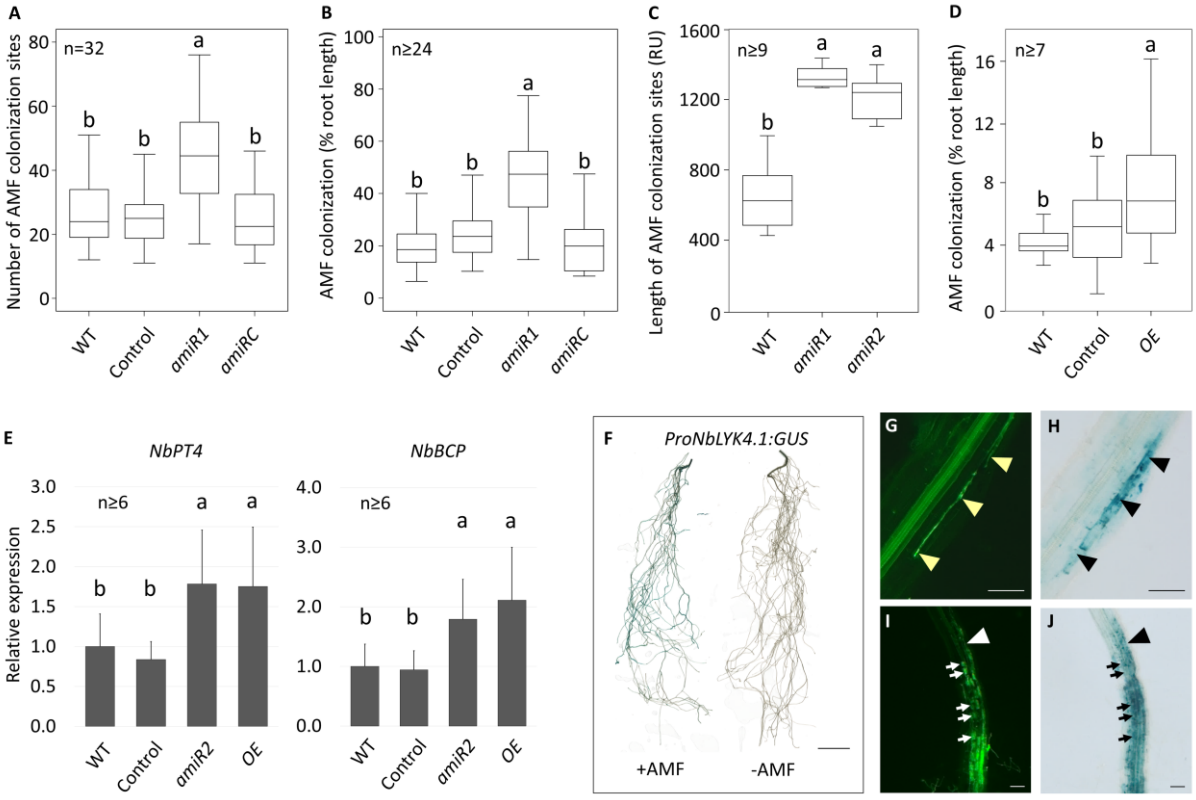

Figure 4. *NbLYK4* regulates AM symbiosis

(A-B) AMF colonization is increased in *NbLYK4*-silenced plants. The entire *N. benthamiana* root systems were stained by ink 3 wpi (A) or 4 wpi (B) with *Rhizophagus irregularis*. Box plots represent the number of AMF colonization sites (A) or the percentage of root length colonization (B) in a total of 24 to 32 plants from two independent experiments. Center lines show the medians, box limits the upper and lower quartiles, and whiskers 1.5x the interquartile range. The different letters indicate significant differences between the lines ($P < 0.05$, Kruskal-Wallis test). **(C)** Length of colonization sites is increased in *NbLYK4*-silenced plants at 3 wpi. At least 10 colonization sites / plant were randomly imaged and their length (in the root axis) was measured using ImageJ (Relative units, RU). Box plots represent the mean colonization site length / plant in 9 to 10 plants / line. Box plots as in A-B. The different letters indicate significant differences between the lines ($P < 0.05$, Pairwise T-Test). **(D)** AMF colonization is increased in lines overexpressing *NbLYK4* (OE) at 4 wpi. Box plots represent the percentage of root length colonization in a total of 7 to 20 plants from one experiment. Box plots as in A-B. The data from two independent transgenic lines overexpressing *NbLYK4.1* or *NbLYK4.2* (OE) were pooled. The different letters indicate significant differences between the lines ($P < 0.05$, Pairwise T-Test). **(E)** Relative expression of the plant AM-marker genes in the indicated *N. benthamiana* lines measured by RT-qPCR. RNAs were extracted from pools of

three root systems. Means and standard deviations between at least 6 samples from three independent experiments are shown. The data from two independent OE lines were pooled. The different letters indicate significant differences between the lines ($P < 0.05$, Pairwise T-Test). **(F)** *NbLYK4* expression is induced by AMF colonization. GUS activity (blue) is detected in a transgenic *ProNbLYK4.1:GUS* line grown in axenic conditions only when inoculated by *R. irregularis*. **(G-J)** *NbLYK4* expression is induced by growing AMF hyphae. GUS activity (blue, H and J) in root segments of a *ProNbLYK4.1:GUS* line containing *R. irregularis* hyphae (arrowheads) and arbuscules (arrows) stained by WGA-CF488A (green, G and I). Scale bars represent 1cm in F and 100µm in G-I.

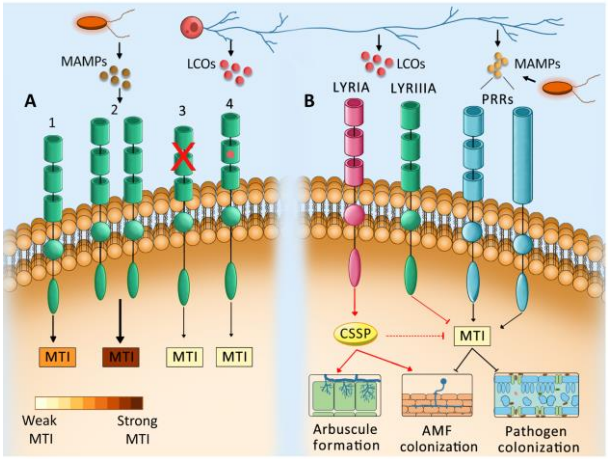

Figure 5. Model for LYRIIIA mode of action.

(A) Basal expression of LysM-RLK LYRIIIA proteins constitutively activates microbe-associated molecular patterns (MAMP)-triggered immunity (MTI, 1). In presence of microbes, LYRIIIA expression is induced leading to increased defense responses (2). In knock-down and knock-out mutants, constitutive activation of MTI by LYRIIIA proteins is lost leading to a decreased defense responses (3). Lipo-chitooligosaccharide (LCO) binding might abolish constitutive activation of MTI (4). **(B)** Pathogens and arbuscular mycorrhizal fungi (AMF) produce MAMPs that activate MTI through pattern recognition receptors (PRRs) and decrease their ability to colonize. AMF also produces LCOs that are perceived by LYRIA and LYRIIIA proteins. Both can modulate MTI (dashed line, only shown in *M. truncatula*). LYRIA proteins are also involved in AMF colonization and arbuscule formation through activating the common symbiosis signaling pathway (CSSP).

REFERENCES

Anders, S., and Huber, W. (2010). Differential expression analysis for sequence count data. Genome Biol **11,** R106.

Arrighi, J.F., Barre, A., Ben Amor, B., Bersoult, A., Soriano, L.C., Mirabella, R., de Carvalho-Niebel, F., Journet, E.P., Ghérardi, M., Huguet, T., Geurts, R., Dénarié, J., Rougé, P., and Gough, C. (2006). The Medicago truncatula lysin motif-receptor-like kinase gene family includes NFP and new nodule-expressed genes. Plant Physiol **142,** 265-279.

Ben, C., Toueni, M., Montanari, S., Tardin, M.C., Fervel, M., Negahi, A., Saint-Pierre, L., Mathieu, G., Gras, M.C., Noël, D., Prospéri, J.M., Pilet-Nayel, M.L., Baranger, A., Huguet, T., Julier, B., Rickauer, M., and Gentzbittel, L. (2013). Natural diversity in the model legume Medicago truncatula allows identifying distinct genetic mechanisms conferring partial resistance to Verticillium wilt. J Exp Bot **64,** 317-332.

Broghammer, A., Krusell, L., Blaise, M., Sauer, J., Sullivan, J.T., Maolanon, N., Vinther, M., Lorentzen, A., Madsen, E.B., Jensen, K.J., Roepstorff, P., Thirup, S., Ronson, C.W., Thygesen, M.B., and Stougaard, J. (2012). Legume receptors perceive the rhizobial lipochitin oligosaccharide signal molecules by direct binding. Proc Natl Acad Sci USA **109,** 13859-13864.

Buendia, L., Wang, T., Girardin, A., and Lefebvre, B. (2016). The LysM receptor-like kinase SlLYK10 regulates the arbuscular mycorrhizal symbiosis in tomato. New Phytol **210,** 184-195.

Buendia, L., Girardin, A., Wang, T., Cottret, L., and Lefebvre, B. (2018). LysM Receptor-Like Kinase and LysM Receptor-Like Protein Families: An Update on Phylogeny and Functional Characterization. Front Plant Sci **9,** 1531.

B**ouchiba, Y., J. Esque, L. Cottret, M. Maréchaux, M. Gaston, V. Gasciolli, J. Keller, N. Nouwen, D. Gully, J. F. Arrighi, C. Gough, B. Lefebvre, S. Barbe and J. J. Bono** (2022). An integrated approach reveals how lipo-chitooligosaccharides interact with the lysin motif receptor-like kinase MtLYR3. Protein Sci 31: e4327.

Campos-Soriano, L., Garcia-Martinez, J., and Segundo, B.S. (2012). The arbuscular mycorrhizal symbiosis promotes the systemic induction of regulatory defence-related genes in rice leaves and confers resistance to pathogen infection. Mol Plant Pathol **13,** 579-592.

Cao, Y., Liang, Y., Tanaka, K., Nguyen, C.T., Jedrzejczak, R.P., Joachimiak, A., and Stacey, G. (2014). The kinase LYK5 is a major chitin receptor in Arabidopsis and forms a chitin-induced complex with related kinase CERK1. Elife **3,** e03766.

Chen, M., Bruisson, S., Bapaume, L., Darbon, G., Glauser, G., Schorderet, M., and Reinhardt, D. (2021). VAPYRIN attenuates defence by repressing PR gene induction and localized lignin accumulation during arbuscular mycorrhizal symbiosis of Petunia hybrida. New Phytol **229**, 3481-3496.

Cheval, C., Samwald, S., Johnston, M.G., de Keijzer, J., Breakspear, A., Liu, X., Bellandi, A., Kadota, Y., Zipfel, C., and Faulkner, C. (2020). Chitin perception in plasmodesmata characterizes submembrane immune-signaling specificity in plants. Proc Natl Acad Sci USA **117,** 9621-9629.

Chinchilla, D., Bauer, Z., Regenass, M., Boller, T., and Felix, G. (2006). The Arabidopsis receptor kinase FLS2 binds flg22 and determines the specificity of flagellin perception. Plant Cell **18,** 465-476.

Del Hierro, I., Mélida, H., Broyart, C., Santiago, J., and Molina, A. (2021). Computational prediction method to decipher receptor-glycoligand interactions in plant immunity. Plant J, 105: 1710-1726.

Delaux, P., Varala, K., Edger, P., Coruzzi, G., Pires, J., and Ane, J. (2014). Comparative Phylogenomics Uncovers the Impact of Symbiotic Associations on Host Genome Evolution. Plos Genetics **10,** e1004487.

Denoux, C., Galletti, R., Mammarella, N., Gopalan, S., Werck, D., De Lorenzo, G., Ferrari, S., Ausubel, F.M., and Dewdney, J. (2008). Activation of defense response pathways by OGs and Flg22 elicitors in Arabidopsis seedlings. Mol Plant **1,** 423-445.

Feng, F., Sun, J., Radhakrishnan, G.V., Lee, T., Bozsóki, Z., Fort, S., Gavrin, A., Gysel, K., Thygesen, M.B., Andersen, K.R., Radutoiu, S., Stougaard, J., and Oldroyd, G.E.D. (2019). A combination

of chitooligosaccharide and lipochitooligosaccharide recognition promotes arbuscular mycorrhizal associations in Medicago truncatula. Nat Commun **10,** 5047.

Fiorilli, V., Vannini, C., Ortolani, F., Garcia-Seco, D., Chiapello, M., Novero, M., Domingo, G., Terzi, V., Morcia, C., Bagnaresi, P., Moulin, L., Bracale, M., and Bonfante, P. (2018). Omics approaches revealed how arbuscular mycorrhizal symbiosis enhances yield and resistance to leaf pathogen in wheat. Sci Rep **8**, 9625.

Fliegmann, J., and Bono, J.J. (2015). Lipo-chitooligosaccharidic nodulation factors and their perception by plant receptors. Glycoconj J **32,** 455-464.

Fliegmann, J., Jauneau, A., Pichereaux, C., Rosenberg, C., Gasciolli, V., Timmers, A.C., Burlet-Schiltz, O., Cullimore, J., and Bono, J.J. (2016). LYR3, a high-affinity LCO-binding protein of Medicago truncatula, interacts with LYK3, a key symbiotic receptor. FEBS Lett **590,** 1477-1487.

Fliegmann, J., Canova, S., Lachaud, C., Uhlenbroich, S., Gasciolli, V., Pichereaux, C., Rossignol, M., Rosenberg, C., Cumener, M., Pitorre, D., Lefebvre, B., Gough, C., Samain, E., Fort, S., Driguez, H., Vauzeilles, B., Beau, J.-M., Nurisso, A., Imberty, A., Cullimore, J., and Bono, J.-J. (2013). Lipo-chitooligosaccharidic Symbiotic Signals Are Recognized by LysM Receptor-Like Kinase LYR3 in the Legume Medicago truncatula. ACS Chemical Biology **8,** 1900-1906.

Fuechtbauer, W., Yunusov, T., Bozsóki, Z., Gavrin, A., James, E.K., Stougaard, J., Schornack, S., and Radutoiu, S. (2018). LYS12 LysM receptor decelerates Phytophthora palmivora disease progression in Lotus japonicus. Plant J **93,** 297-310.

Girardin, A., Wang, T., Ding, Y., Keller, J., Buendia, L., Gaston, M., Ribeyre, C., Gasciolli, V., Auriac, M.C., Vernié, T., Bendahmane, A., Ried, M.K., Parniske, M., Morel, P., Vandenbussche, M., Schorderet, M., Reinhardt, D., Delaux, P.M., Bono, J.J., and Lefebvre, B. (2019). LCO Receptors Involved in Arbuscular Mycorrhiza Are Functional for Rhizobia Perception in Legumes. Curr Biol **29,** 4249-4259.e4245.

Gomez-Gomez, L., and Boller, T. (2000). FLS2: an LRR receptor-like kinase involved in the perception of the bacterial elicitor flagellin in Arabidopsis. Mol Cell **5,** 1003-1011.

Güimil, S., Chang, H.S., Zhu, T., Sesma, A., Osbourn, A., Roux, C., Ioannidis, V., Oakeley, E.J., Docquier, M., Descombes, P., Briggs, S.P., and Paszkowski, U. (2005). Comparative transcriptomics of rice reveals an ancient pattern of response to microbial colonization. Proc Natl Acad Sci USA **102,** 8066-8070.

Hann, D.R., and Rathjen, J.P. (2007). Early events in the pathogenicity of Pseudomonas syringae on Nicotiana benthamiana. Plant J **49,** 607-618.

Hao, G., Pitino, M., Duan, Y., and Stover, E. (2016). Reduced Susceptibility to Xanthomonas citri in Transgenic Citrus Expressing the FLS2 Receptor From Nicotiana benthamiana. Mol Plant Microbe Interact **29,** 132-142.

He, J., Zhang, C., Dai, H., Liu, H., Zhang, X., Yang, J., Chen, X., Zhu, Y., Wang, D., Qi, X., Li, W., Wang, Z., An, G., Yu, N., He, Z., Wang, Y.F., Xiao, Y., Zhang, P., and Wang, E. (2019). A LysM Receptor Heteromer Mediates Perception of Arbuscular Mycorrhizal Symbiotic Signal in Rice. Mol Plant.

Kloppholz, S., Kuhn, H., and Requena, N. (2011). A Secreted Fungal Effector of Glomus intraradices Promotes Symbiotic Biotrophy. Curr Biol **21,** 1204-1209.

Lefebvre, B., Klaus-Heisen, D., Pietraszewska-Bogiel, A., Herve, C., Camut, S., Auriac, M.-C., Gasciolli, V., Nurisso, A., Gadella, T.W.J., and Cullimore, J. (2012). Role of N-Glycosylation Sites and CXC Motifs in Trafficking of Medicago truncatula Nod Factor Perception Protein to Plasma Membrane. J Biol Chem **287,** 10812-10823.

Lefebvre, B., Timmers, T., Mbengue, M., Moreau, S., Herve, C., Toth, K., Bittencourt-Silvestre, J., Klaus, D., Deslandes, L., Godiard, L., Murray, J.D., Udvardi, M.K., Raffaele, S., Mongrand, S., Cullimore, J., Gamas, P., Niebel, A., and Ott, T. (2010). A remorin protein interacts with symbiotic receptors and regulates bacterial infection. Proc Natl Acad Sci USA **107,** 2343-2348.

Li, H., Handsaker, B., Wysoker, A., Fennell, T., Ruan, J., Homer, N., Marth, G., Abecasis, G., Durbin, R., and Subgroup, G.P.D.P. (2009). The Sequence Alignment/Map format and SAMtools. Bioinformatics **25,** 2078-2079.

Liang, Y., Cao, Y., Tanaka, K., Thibivilliers, S., Wan, J., Choi, J., Kang, C., Qiu, J., and Stacey, G. (2013). Nonlegumes Respond to Rhizobial Nod Factors by Suppressing the Innate Immune Response. Science **341,** 1384-1387.

Liao, Y., Smyth, G.K., and Shi, W. (2014). featureCounts: an efficient general purpose program for assigning sequence reads to genomic features. Bioinformatics **30,** 923-930.

Love, M.I., Huber, W., and Anders, S. (2014). Moderated estimation of fold change and dispersion for RNA-seq data with DESeq2. Genome Biol **15,** 550.

Lyons, R., Iwase, A., Gänsewig, T., Sherstnev, A., Duc, C., Barton, G.J., Hanada, K., Higuchi-Takeuchi, M., Matsui, M., Sugimoto, K., Kazan, K., Simpson, G.G., and Shirasu, K. (2013). The RNA-binding protein FPA regulates flg22-triggered defense responses and transcription factor activity by alternative polyadenylation. Sci Rep **3,** 2866.

Madsen, E.B., Madsen, L.H., Radutoiu, S., Olbryt, M., Rakwalska, M., Szczyglowski, K., Sato, S., Kaneko, T., Tabata, S., Sandal, N., and Stougaard, J. (2003). A receptor kinase gene of the LysM type is involved in legume perception of rhizobial signals. Nature **425,** 637-640.

Maillet, F., Poinsot, V., André, O., Puech-Pagès, V., Haouy, A., Gueunier, M., Cromer, L., Giraudet, D., Formey, D., Niebel, A., Martinez, E.A., Driguez, H., Bécard, G., and Dénarié, J. (2011). Fungal lipochitooligosaccharide symbiotic signals in arbuscular mycorrhiza. Nature **469,** 58-63.

Malkov, N., Fliegmann, J., Rosenberg, C., Gasciolli, V., Timmers, A.C., Nurisso, A., Cullimore, J., and Bono, J.J. (2016). Molecular basis of lipo-chitooligosaccharide recognition by the lysin motif receptor-like kinase LYR3 in legumes. Biochem J **473,** 1369-1378.

Mbengue, M., Camut, S., de Carvalho-Niebel, F., Deslandes, L., Froidure, S., Klaus-Heisen, D., Moreau, S., Rivas, S., Timmers, T., Herve, C., Cullimore, J., and Lefebvre, B. (2010). The Medicago truncatula E3 Ubiquitin Ligase PUB1 Interacts with the LYK3 Symbiotic Receptor and Negatively Regulates Infection and Nodulation. Plant Cell **22,** 3474-3488.

Miya, A., Albert, P., Shinya, T., Desaki, Y., Ichimura, K., Shirasu, K., Narusaka, Y., Kawakami, N., Kaku, H., and Shibuya, N. (2007). CERK1, a LysM receptor kinase, is essential for chitin elicitor signaling in Arabidopsis. Proc Natl Acad Sci USA **104,** 19613-19618.

Miyata, K., Hayafune, M., Kobae, Y., Kaku, H., Nishizawa, Y., Masuda, Y., Shibuya, N., and Nakagawa, T. (2016). Evaluation of the Role of the LysM Receptor-Like Kinase, OsNFR5/OsRLK2 for AM Symbiosis in Rice. Plant Cell Physiol **57,** 2283-2290.

Mortazavi, A., Williams, B.A., McCue, K., Schaeffer, L., and Wold, B. (2008). Mapping and quantifying mammalian transcriptomes by RNA-Seq. Nat Methods **5,** 621-628.

Plener, L., Manfredi, P., Valls, M., and Genin, S. (2010). PrhG, a transcriptional regulator responding to growth conditions, is involved in the control of the type III secretion system regulon in Ralstonia solanacearum. J Bacteriol **192,** 1011-1019.

Poueymiro, M., Cunnac, S., Barberis, P., Deslandes, L., Peeters, N., Cazale-Noel, A.C., Boucher, C., and Genin, S. (2009). Two type III secretion system effectors from Ralstonia solanacearum GMI1000 determine host-range specificity on tobacco. Mol Plant Microbe Interact **22,** 538-550.

Rasmussen, S.R., Füchtbauer, W., Novero, M., Volpe, V., Malkov, N., Genre, A., Bonfante, P., Stougaard, J., and Radutoiu, S. (2016). Intraradical colonization by arbuscular mycorrhizal fungi triggers induction of a lipochitooligosaccharide receptor. Sci Rep **6,** 29733.

Remigi, P., Anisimova, M., Guidot, A., Genin, S., and Peeters, N. (2011). Functional diversification of the GALA type III effector family contributes to Ralstonia solanacearum adaptation on different plant hosts. New Phytol **192,** 976-987.

Rey, T., André, O., Nars, A., Dumas, B., Gough, C., Bottin, A., and Jacquet, C. (2019). Lipo-chitooligosaccharide signalling blocks a rapid pathogen-induced ROS burst without impeding immunity. New Phytol **221,** 743-749.

Rey, T., Nars, A., Bonhomme, M., Bottin, A., Huguet, S., Balzergue, S., Jardinaud, M.F., Bono, J.J., Cullimore, J., Dumas, B., Gough, C., and Jacquet, C. (2013). NFP, a LysM protein controlling Nod factor perception, also intervenes in Medicago truncatula resistance to pathogens. New Phytol **198,** 875-886.

Rich, M.K., Schorderet, M., Bapaume, L., Falquet, L., Morel, P., Vandenbussche, M., and Reinhardt, D. (2015). The Petunia GRAS Transcription Factor ATA/RAM1 Regulates Symbiotic Gene Expression and Fungal Morphogenesis in Arbuscular Mycorrhiza. Plant Physiol **168**, 788-797.

Robinson, M.D., McCarthy, D.J., and Smyth, G.K. (2010). edgeR: a Bioconductor package for differential expression analysis of digital gene expression data. Bioinformatics **26,** 139-140.

Rush, T.A., Puech-Pagès, V., Bascaules, A., Jargeat, P., Maillet, F., Haouy, A., Maës, A.Q., Carriel, C.C., Khokhani, D., Keller-Pearson, M., Tannous, J., Cope, K.R., Garcia, K., Maeda, J., Johnson, C., Kleven, B., Choudhury, Q.J., Labbé, J., Swift, C., O'Malley, M.A., Bok, J.W., Cottaz, S., Fort, S., Poinsot, V., Sussman, M.R., Lefort, C., Nett, J., Keller, N.P., Bécard, G., and Ané, J.M. (2020). Lipo-chitooligosaccharides as regulatory signals of fungal growth and development. Nat Commun **11,** 3897.

Schultink, A., Qi, T., Lee, A., Steinbrenner, A.D., and Staskawicz, B. (2017). Roq1 mediates recognition of the Xanthomonas and Pseudomonas effector proteins XopQ and HopQ1. Plant J **92,** 787-795.

Shaw, S.L., and Long, S.R. (2003). Nod factor inhibition of reactive oxygen efflux in a host legume. Plant Physiol **132,** 2196-2204.

Wan, J., Tanaka, K., Zhang, X., Son, G., Brechenmacher, L., Tran, H., and Stacey, G. (2012). LYK4, a Lysin Motif Receptor-Like Kinase, Is Important for Chitin Signaling and Plant Innate Immunity in Arabidopsis. Plant Physiol **160,** 396-406.

Wang, L., Wang, S., and Li, W. (2012). RSeQC: quality control of RNA-seq experiments. Bioinformatics **28,** 2184-2185.

Watts-Williams, S.J., Emmett, B.D., Levesque-Tremblay, V., MacLean, A.M., Sun, X., Satterlee, J.W., Fei, Z., and Harrison, M.J. (2019). Diverse Sorghum bicolor accessions show marked variation in growth and transcriptional responses to arbuscular mycorrhizal fungi. Plant Cell Environ **42,** 1758-1774.

Yu, G., Wang, L.G., Han, Y., and He, Q.Y. (2012). clusterProfiler: an R package for comparing biological themes among gene clusters. OMICS **16,** 284-287.

Zeng, T., Rodriguez-Moreno, L., Mansurkhodzaev, A., Wang, P., van den Berg, W., Gasciolli, V., Cottaz, S., Fort, S., Thomma, B.P.H.J., Bono, J.J., Bisseling, T., and Limpens, E. (2020). A lysin motif effector subverts chitin-triggered immunity to facilitate arbuscular mycorrhizal symbiosis. New Phytol **225,** 448-460.